Received: 3 December 2021 | Revised: 6 March 2022 | Accepted: 12 March 2022

DOI: 10.1002/ldr.4264

RESEARCH ARTICLE

WILEY

Soil water movement differences relating to banana (*Musa nana* Lour.) plantation regime

Wanjun Zhang[1,2] | Xiai Zhu[1,3] | Shuoyang Ji[4] | Chunfeng Chen[1,3] | Huanhuan Zeng[1,3] | Xin Zou[1,3] | Bin Yang[1,3] | Xiaojin Jiang[1,3] | Wenjie Liu[1,3]

[1]CAS Key Laboratory of Tropical Forest Ecology, Xishuangbanna Tropical Botanical Garden, Chinese Academy of Sciences, Menglun, PR China

[2]Key Laboratory of Vegetation Restoration and Management of Degraded Ecosystems, South China Botanical Garden, Chinese Academy of Sciences, Guangzhou, PR China

[3]Center of Plant Ecology, Core Botanical Gardens, Chinese Academy of Sciences, Menglun, PR China

[4]School of Housing, Building and Planning, University Sains Malaysia, Penang, Malaysia

Correspondence
Wenjie Liu and Xiaojin Jiang, Key Laboratory of Tropical Forest Ecology, Xishuangbanna Tropical Botanical Garden, Chinese Academy of Sciences, Menglun, Mengla, Yunnan 666303, PR China.
Email: lwj@xtbg.org.cn and jiangxiaojin@xtbg.ac.cn

Funding information
National Natural Science Foundation of China, Grant/Award Numbers: 32001221, 41701029; Natural Science Foundation of Yunnan Province, Grant/Award Numbers: 2018FB043, 2018FB076, 202001AU070136, 202101AS070010, 202101AT070056

Abstract

The long-term cultivation of banana crops (*Musa nana* Lour.) has caused improper utilization of soil and water resources. However, the effect of the banana plantation regime on soil water flow pattern is still poorly understood. This study focused on the dominant pattern of soil water movement in the 1-year (B1) and 4-year (B2) old banana plantations. The results showed that: (1) the soil physical properties showed variability with soil depths, especially obvious changes from surface to 40 cm depth, which had restriction on soil infiltration in different depths. (2) The saturated hydraulic conductivity (*Ks*) decreased with the increasing distance from the banana stem. Moreover, the *Ks* in the B2 plot increased by 65.5% compared to the B1 plot at the soil layer 0–20 cm. (3) Preferential flow was the main path of soil water transport and was significantly influenced by soil bulk density, porosity, and root systems. Redundancy analysis (RDA) showed that banana root biomass was the most prominent factor influencing the dyed area. (4) The soil infiltrability and the preferential flow degree of both B1 and B2 plots were stronger in the root zone than those in the non-root zone. Such results were attributed to the root systems around the banana stem that were more developed than those far away from the stem (more accurately pseudostems); a large number of pore channels formed around the root systems that promoted the preferential flow. Or results suggest that banana root was the important factor affecting soil water movement. The improvement in the root network of banana plantation regime can result in better soil physical properties. This knowledge will be vital for the sustainable cultivation and irrigation of banana crops.

KEYWORDS
banana plantation regime, infiltration, preferential flow, root biomass, soil physical properties

1 | INTRODUCTION

Water and soil resources are the crucial for human existence and development, and an important restriction factor of sustainable development of the environment. Generally, landscape conversion, irrigation management, and crop planting patterns can directly affect local water and soil resources, such as soil water redistribution, plant water use, and surface runoff (Wang et al., 2007). For example, no-tillage reduces soil moisture evaporation and drought stress, but may decrease water infiltration, and increasing surface hardening; Deep tillage increases soil porosity, which is conducive to water infiltration, but increases the risk of soil erosion (Martinez et al., 2008). In addition, the roots of monocropping or short-term cropping systems are less developed than those of composite or long-term cropping systems, which can also change soil structure and affect soil water movement (Lipiec et al., 2006). Consequently, the allocation of soil water

resources can affect soil water flow paths, groundwater recharge, and plant water and nutrient utilization. Good ecological environment, especially water and soil environment, is the basis of increasing crop yield and economic benefits in the plantations. Therefore, the study of soil water movement is helpful to the planning of reasonable irrigation and tillage methods, and the understanding of local hydrologic processes.

In general, due to the heterogeneity of soil physical properties (e.g., porosity, bulk density), water movement through soil is not uniform, but the combination of preferential and matrix flows (Allaire et al., 2009; Beven & Germann, 2013). Matrix flow refers to the slow and uniform flow of water and solute in soil, while preferential flow refers to the more rapid movement of water and solute along pore channels (Gazis & Feng, 2004), mainly including macropore flow, bypass flow, finger flow, and lateral flow (Hardie et al., 2011). The existence of preferential flow has a significant influence on the formation mechanism of surface runoff and ground water, which is influenced by many factors, such as soil bulk density, porosity, plant root activity, and animal burrows (Bromley et al., 1997; Zhu et al., 2019). Plant roots play a crucial role in improving soil properties and water infiltration, due to their activity, including the living roots embedding, entangling, and enwrapping in soil (Ludwig et al., 2005; Niemeyer et al., 2014). For instance, Jiang et al. (2019) found that the non-capillary porosity near root zones was significantly greater than those in the non-root zone. The channels formed by plant roots can support deeper water infiltration, accelerating the preferential flow process (Jiang et al., 2018; Wine et al., 2012), and promoting rapid solute transport at the same time (Jørgensen et al., 2002).

In order to quantify the preferential flow pattern, dye-tracer techniques have been used to visualize the flow paths of soil water, and several studies have clearly shown that it is a reliable technique with high spatial resolution to explain complex water movements (Bouma et al., 1977; Ghodrati & Jury, 1990). In spite of this, Flury et al. (1994) recognized early on the disadvantages of dye-tracer techniques like destructive sampling and the non-repeatability of samples, which would inevitably lead to large errors. From the 20th century to the present, however, the preferential flow sampling has still concentrated on a small scale, that is, on the point scale. Only a single dye section is collected to obtain a small range of preferential flow paths, which obviously cannot fully demonstrate the large-scale pattern of soil water movement. Plot-scale dye experiments in several previous studies (e.g., Öhrström et al., 2002) have suggested that larger scale dyeing greater than point scales were helpful in visualizing the real water flow pathways. Therefore, it is necessary to construct dyeing plots on a larger spatial scale and to sample from multiple soil profiles in order to obtain preferential flow paths.

Bananas (*Musa nana* Lour.) are widely cultivated in the high temperature and rainy areas of tropical and subtropical regions all over the world. Due to the natural conditions, the Xishuangbanna area (Southwest China) is one of the most suitable areas of the Country for banana cultivation. From 2001 to 2015, the cultivated area of bananas increased rapidly from 500 to 26733.3 ha, accounting for about 25.9% of the total area in China (People's Government of Xishuangbanna, 2018). Heavy application of chemical fertilizers, pesticides, and irrigation in banana plantations has disturbed the soil environment. Rapid water infiltration and preferential flow activities can effectively respond to water input and mitigate runoff deterioration and soil erosion. However, the basic characteristics of soil properties and water transport in banana plantations are unknown yet, which hinders the understanding of the soil hydrological process and restricts the analysis of soil and water loss. Therefore, in this study, we selected two banana plantations with different planting years for soil water movement research, the specific objectives were to: (1) investigate soil water movement characteristics for different banana planting ages; and (2) reveal how changes in preferential flow were associated with soil properties. We hypothesized that: (i) soil infiltrability and water movement pattern would vary with different planting regimes; (ii) soil preferential flow degree was closely associated with the macropores generated by banana root systems and soil physical properties.

2 | MATERIALS AND METHODS

2.1 | Site description

The study site was located in the Xishuangbanna Tropical Botanical Garden (XTBG; 21°55′39″ N, 101°15′55″ E; 570–600 m asl), Mengla County, Yunnan Province, Southwest China. The local climate is dominated by the southern tropical monsoons from the Indian Ocean during the rainy season (from May to October), and controlled at its southern edges by the subtropical jet streams that prevail and delivers dry hot and cold air during the dry season (from November to February). According to the climate in the past 40 years, the mean annual air temperature and precipitation were 21.7°C and 1480 mm, respectively; approximately 87% of the annual total precipitation occurs during the rainy season and 13% during the dry season. According to the classification system of the International Union of Soil Scientists, based on the clay content, <15% are sandy texture and loam texture; 15% ∼ 25% are clay-loam groups; > 25% are clay. In this study area, the soil has a clay-loam texture (56% sand, 27% silt, and 17% clay).

This study was conducted in a 4.3-ha plot, where the land was transformed banana plantation from a rubber monoculture 6 years before. Two different age banana plantations were used as measuring plots, 1-year- and 4-year-old, being 100 m apart and both planted at a density of 5000 banana plantains/ha. Mature banana bunches are harvested between April and May at three growth stages: vegetative, flowering, and fruit appearance. After harvest, the pseudostems are chopped down and the new banana shoots that sprouted from the parent plantain grow rapidly. The two banana plantations studied during our experimental period were both at the flowering stage. In general, banana plantations are frequently irrigated to meet the demand for water during the dry period, while the irrigation amount in banana plantations is not scientifically planned by farmers. The banana plantations was managed through application of fertilizers, and weeding and pest control (pesticide spraying) were performed throughout the year.

2.2 | Soil physical properties

Experiments were conducted in three plots: no vegetation (NV plot), 1-year banana plantation (B1 plot) and 4-year banana plantation (B2 plot). Bulk soil samples were used for the measurement of soil physical properties (Danielson & Sutherland, 1986). In each plot, bulk soil samples were collected at five depths of 0–20, 20–40, 40–60, 60–80, and 80–100 cm using cutting cylinders (volume, 200.0 cm^3), in three repetitions. In the laboratory, soil samples were placed in distilled water for saturation. Twenty-four hr being pounded, the saturated soil water was weighed (W_{sat}, g). Then, the saturated samples were placed on the sand to measure the weight of water drained through gravity after 2 hr (W_{2h}) and 4 days (W_{4d}). Finally, the weight of the cutting cylinder containing dry soil (W_{dry}) was measured after oven drying at 105°C for 24 hr. Soil total porosity was calculated in undisturbed water-saturated samples of 200 cm^3 on the assumption that no air was trapped in the pores and validated using dry bulk density and a particle density of 2.65 g cm^{-3} (Danielson & Sutherland, 1986). Then, initial water content (*IWC*), bulk density (*BD*), total porosity (*TP*), capillary porosity (*CP*), non-capillary porosity (*NCP*), field water capacity (*FWC*) were determined with the following formulae:

$$IWC\,(\%) = \frac{W_{wet} - W_{dry}}{W_{dry} - W_{emp}} \times 100\% \quad (1)$$

$$BD\,(g\,cm^{-3}) = \frac{W_{dry} - W_{emp}}{200\,(cm^3)} \quad (2)$$

$$TP\,(\%) = \left(1 - \frac{BD}{2.65}\right) \times 100\% \quad (3)$$

$$CP\,(\%) = \frac{W_{2h} - W_{dry}}{200 \times \rho_{water}} \times 100\% \quad (4)$$

$$NCP\,(\%) = (TP - CP) \times 100\% \quad (5)$$

$$FWC\,(\%) = \frac{W_{4d} - W_{dry}}{W_{dry} - W_{emp}} \times 100\% \quad (6)$$

Where: the weights of the empty cutting cylinder and the cutting cylinder containing initial wet soil were recorded as W_{emp} and W_{wet} (*g*).

2.3 | Infiltration measurement

The soil saturated hydraulic conductivity was measured at depths of 0–20, 20–40, 40–60, 60–80, and 80–100 cm using the stainless-steel cylinders (inner diameter, 10.0 cm; height, 20.0 cm). Each cylinder was driven into the soil, leaving the height 10.0 cm above the soil surface, and a reference ruler was attached on the inner wall to measure the depth of water infiltrating. The cylinder was initially filled with water equivalent to a water head of 10.0 cm, and the reduced water level height was recorded at 2-min intervals for 20 min and then at 5 min intervals for at least 40 min. The initial infiltration rate (*IIR*, mm min^{-1}) was defined as the ratio of the reduced water depth to the initial infiltration time (2 min). Each cylinder was rapidly refilled to a height of 10.0 cm after each recording until the difference in water level between filling and after 5 min remained the same for five consecutive times. The water refilling procedure of infiltration took approximately 1.0 hr. We assumed that a steady-state flow occurred at this point, and the actual steady-state infiltration rate (*Is*, mm min^{-1}) was calculated based on the last five measured values (Bodhinayake et al., 2004). Due to water temperature affecting *Is*, the *Is* was converted to the quasi-steady infiltrate rate (*SIR*, mm min^{-1}) at 10°C, and the *SIR* was used to calculate the soil saturated hydraulic conductivity (*Ks*, cm min^{-1}) (Reynolds & Elrick, 1990):

$$SIR = \frac{I_s}{0.7 + 0.03T} \quad (7)$$

$$Ks = \frac{SIR}{\frac{H_s}{C_1 d_s + C_2 r_s} + \frac{1}{S(C_1 d_s + C_2 r_s)} + 1} \quad (8)$$

Where: $T = 20$°C indicates the actual water temperature of *Is* state; $C_1 = 0.316\pi$ and $C_2 = 0.184\pi$ are dimensionless constants. H_s is the height (10.0 cm) of water inside the cylinder, d_s is the rest of the height (10 cm) of cylinder, r_s is the radius of the cylinder, and *S* is the sorptive number (12 cm^{-1}).

2.4 | Dye-tracer experiment

The micro-zone dye-tracer experiment was carried out using brilliant blue FCF in NV, B1, and B2. In both B1 and B2 plots, a 2 × 2 m square plot around a single banana stem was built using corrugated-iron sheet. As a control experiment, there was no vegetation cover in the NV plot, and a 1 × 1 m square plot was built. Before dyeing, it is necessary to clear up the dyeing plots and to level the topsoil. Dissolving 680 g of bright blue dye in 180 L of water, for brilliant blue FCF dye solution with a concentration of 4.0 g L^{-1}. 80 L solution was injected into the B1 plot and B2 plot, respectively and 20 L solution was injected into the NV plot (equivalent to 20 mm irrigation or rainfall amount). After 24 hr, 8 soil dyeing profiles in the B1 and B2 plots were taken 20 cm apart (160 cm width × 120 cm depth); in the NV plot, 8 soil profiles were taken 10 cm apart (80 cm width × 60 cm depth) (Figure 1). Two scales were placed horizontally and vertically on each soil profile, and then each soil profile was photographed and recorded using a Sony 6000 (Japan) camera. Combined with the corresponding scale of the image processing software and the field profile, the image of the dyed profile was corrected.

The dyeing images were processed using Software ARC MAP 10.3 (ESRI Inc., Redlands, California, USA). Firstly, the pictures of soil profiles were geometrically corrected; secondly, according to the previous studies (Weiler & Hannes, 2004), the dyeing areas were classified into three types of concentrations by the supervised classification: dark (high concentration), moderate (moderate

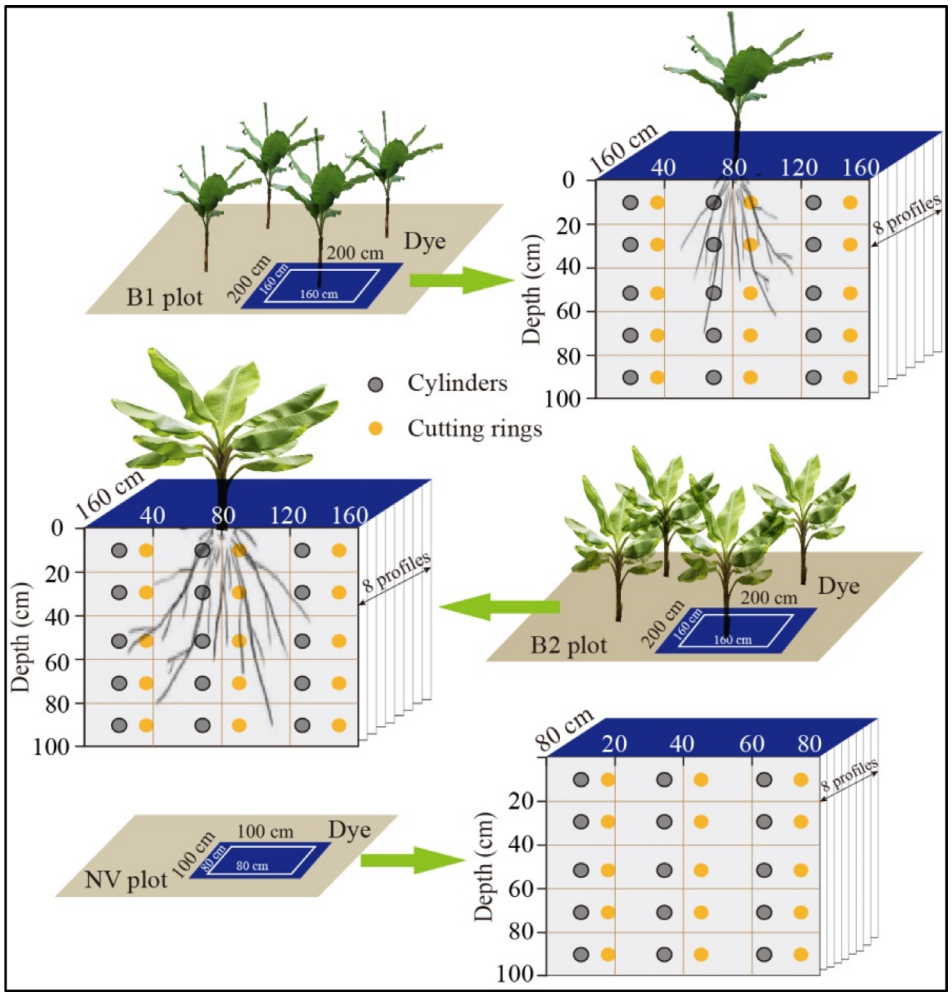

FIGURE 1 Diagram of the experimental design. Dye tracing infiltration test, bulk soil sampling and root biomass sampling in 1-year-old banana plantation (B1) plot and 4-year-old banana plantation (B2) plot and a control test in no vegetation (NV) plot were conducted, respectively. The assumed banana root systems were drawn in the soil profiles [Colour figure can be viewed at wileyonlinelibrary.com]

concentration), and light (low concentration) dyeing area. The dark area indicates the strong macropore flow paths that is heavily stained; the moderate area and light area indicate the strong and weak interactions, respectively, between the macropore flow and the surrounding matrix flow (Jiang et al., 2015). In order to calculate the area of three concentrations per soil depth, grid was created and the dyed profile was divided into pixels (2 × 2 cm). In addition, the 80 cm (width) × 120 cm (depth) the dyed image per soil profiles were separated from the total image to calculate preferential flow indices. The dyeing coverage rate (*DC*, %), coefficient of variation (*CV*, %), uniform infiltration depth (*UID*, cm), and preferential flow fraction (*Pf-r*, %) were calculated (Flury et al., 1994; van Schaik, 2009).

$$DC = \frac{S_{dye}}{S} \times 100\% \quad (9)$$

$$CV = \frac{DC_{std}}{\overline{DC}} \times 100\% \quad (10)$$

$$Pf - r = \left(1 - \frac{UID \times W}{S}\right) \times 100\% \quad (11)$$

Where: S_{dye} is the dye-stained area (cm^2), and *S* is the total profile area (cm^2), dye-stained area plus non-strained area; DC_{std} is the standard error, $\overline{DC}$ is the mean value; *UID* is the depth at which the *DC* decreases below 80%, indicating the depth to which matrix flow is prevalent; *W* is the soil profile width 80 cm.

2.5 | Other relevant measurements

After photographing and recording, each dyed soil profile was divided into 20 × 20 cm square grids in the B1 and B2 plots. Root and soil samples were taken in order to evaluate the relationships between dyed area and root biomass and soil physical properties. Root excavated: at least three dyeing grids were randomly selected at each dyeing soil profile; the grid soil blocks were excavated; a total of 65 root samples were picked and brought back to the laboratory. Root surface was washed and water was removed from the surface with absorbent paper. Roots were classified in three groups based on the diameter: thickness (>3 mm); medium (1–3 mm); and fine (<1 mm). After drying in the oven at 85°C for 24 hr to constant weight, roots were weighed using a balance to obtain root biomass (± 0.01 g). In the B2 plot, soil samples at each dyeing soil profile were randomly taken using cutting cylinders. A total of 75 soil samples were taken to the laboratory for determining soil bulk density and porosity.

In addition, in order to estimate the response of soil moisture to rainfall events, volumetric water content (VWC) was continuously monitored using four soil moisture sensors (HOBO, S-SMC-M005). Two sensors A and B were installed at soil depth 10 cm at a distance of 20 and 100 cm from the banana stem, respectively; sensors C and D were installed at soil depth 40 cm and were perpendicular to sensor A and B, respectively. In order to understand the spatial distribution of the surface soil water infiltration, a total of 30 infiltration rings were arranged around a single banana stem in a 2 × 2 m square plot in the B2 plot.

2.6 | Data analysis

All the data were first tested for normal distribution with 95% confidence bounds. A log-transformation or square root transformation was applied for non-normally distributed data. The spatial distributions of soil property variables were based on kriging method. One-way analysis of variance (ANOVA) was applied to assess the differences in soil properties in SPSS 20.0. Differences among soil depths and sampling plots in the soil properties were analyzed using general linear models with 'depth' and 'plot' as fixed effects in SPSS 20.0. When results were significant, differences among groups were compared using a post hoc Tukey's test. Differences were considered significant at p <0.05. Spearman's correlation coefficients were applied to determine the correlation among the soil physical properties. Besides, redundancy analysis (RDA) was widely used to analyze the impact of each driving force by expounding the correlation between response and explanatory variables (Gabarrón et al., 2018; Zhang et al., 2021). In this study, the RDA was performed to evaluate the effect of soil physical properties (explanatory variables) on dyeing indices (response variables).

TABLE 1 Effects of plot type and soil depth on soil physical and hydrological conditions

Depth (cm)	Plot	BD (g cm^{-3})	NCP (%)	CP (%)	FWC (%)
0–20	NV	1.32 (0.03)b	2.60 (0.37)a	47.66 (0.90)b	33.68 (1.70)b
	B1	1.19 (0.03)c	3.50 (0.18)a	51.73 (0.40)a	40.46 (1.42)a
	B2	1.49 (0.04)a	4.69 (0.36)a	39.48 (1.38)c	24.53 (1.13)c
	B2-R	1.46 (0.04)	6.28 (0.66)	40.52 (1.92)	26.09 (2.53)
	B2-NR	1.56 (0.04)	2.51 (1.00)	39.50 (1.78)	23.85 (1.23)
20–40	NV	1.26 (0.03)b	2.60 (0.92)a	49.76 (0.50)a	36.86 (1.99)a
	B1	1.24 (0.02)b	5.01 (0.14)a	48.07 (1.37)a	40.46 (1.64)a
	B2	1.60 (0.04)a	5.54 (0.27)a	33.86 (1.24)b	19.41 (1.07)b
	B2-R	1.58 (0.04)	7.56 (0.63)	34.41 (1.55)	19.87 (1.62)
	B2-NR	1.56 (0.04)	5.01 (1.18)	36.01 (2.00)	21.46 (1.21)
40–60	NV	1.24 (0.02)b	3.63 (1.52)a	50.08 (1.89)a	37.88 (0.78)a
	B1	1.29 (0.02)b	4.36 (0.08)a	47.08 (0.65)a	34.29 (1.87)b
	B2	1.67 (0.03)a	4.03 (0.43)a	33.21 (0.41)b	17.45 (0.22)c
	B2-R	1.66 (0.03)	4.97 (0.97)	33.01 (0.49)	17.91 (0.83)
	B2-NR	1.75 (0.03)	1.33 (0.10)	34.75 (0.39)	16.82 (0.22)
60–80	NV	1.30 (0.01)b	3.16 (0.04)a	47.61 (0.21)a	37.94 (0.18)a
	B1	1.33 (0.02)b	5.32 (0.05)a	44.45 (0.44)b	34.90 (0.54)b
	B2	1.70 (0.02)a	3.58 (0.38)a	32.37 (0.27)c	17.14 (0.09)c
	B2-R	1.67 (0.02)	5.34 (0.31)	33.18 (0.56)	17.35 (0.23)
	B2-NR	1.73 (0.05)	1.61 (1.66)	33.22 (0.17)	15.96 (0.28)
80–100	NV	1.37 (0.00)b	2.65 (0.13)a	45.76 (0.96)a	31.34 (0.73)a
	B1	1.34 (0.02)b	5.98 (0.10)a	43.49 (0.20)b	30.19 (0.40)a
	B2	1.70 (0.02)a	3.42 (0.21)ab	32.54 (0.44)c	16.34 (0.14)b
	B2-R	1.68 (0.02)	5.65 (0.61)	32.32 (0.65)	17.29 (0.52)
	B2-NR	1.75 (0.03)	1.28 (0.91)	33.95 (0.12)	15.28 (0.82)
Summary of ANOVA (P value)					
Depth		<0.001	0.055	<0.001	<0.001
Plot		<0.001	0.040	<0.001	<0.001
Depth × Plot		<0.001	0.902	<0.001	<0.001

Note: mean (± SE), n = 3. NV, open field; B1, 1-year banana field; B2, 4-year banana plantation; B2-R, root area of 4-year banana plantation; B2-NR, non-root area of 4-year banana field. BD, bulk density; NCP, non-capillary porosity; CP, capillary porosity; FWC, field water capacity. The different lower-case letters a, b and c indicate significant differences among three plots (p <0.05)

3 | RESULTS

3.1 | Soil physical properties

Soil physical properties were significantly different among the different soil depths and among the different sampling plots (p <0.001, Table 1). For soil depth, the bulk density (*BD*) increased with increasing soil depth. The non-capillary porosity (*NCP*) reached a maximum at 20–40 cm. The capillary porosity (*CP*) and field water capacity (*FWC*) both decreased gradually with soil depth. For plots, first, the coefficients of variation (*CV*s) of *NCP* in the B2, B1, and NV plots were 51.4%, 31.7%, and 43.8%, respectively. Second, the mean *BD* in the B2 plot was significantly higher than that in the B1 and NV plots; the *BD* in the B1 plot at a soil depth of 0–20 cm was significantly lower than that in the NV plot (p <0.05), but no significant differences were observed below 20 cm (p >0.05). No significant difference was found in the *NCP* among the three plots (p >0.05). By contrast, significant differences were found in the *CP* among the three plots (p <0.001). The *CP* of both the B1 and the NV plots were significantly higher than that of the B2 plot, and *FWC* among the three plots showed a similar result. Thus, the soil physical properties of the B2 plot were inferior to those of the B1 plot, for example, a 27.3% increase in *BD* and a 25.6% decrease in total porosity.

Moreover, soil profiles in the B2 plot were divided into a root zone (B2-R) and a non-root zone (B2-NR) according to banana root distribution. *BD* was slightly lower in the B2-R (1.60 g cm^{-3}) than in the B2-NR (1.67 g cm^{-3}). *NCP* was obviously higher in the B2-R (5.96%) than in the B2-NR (2.0%). Similarly, both *CP* and *FWC* were higher in the B2-R than in the B2-NR. Therefore, the soil physical properties showed evident variations at different soil depths, sampling plots, and root-related zones, respectively.

3.2 | Water infiltration

The water infiltration process is generally represented by an instantaneous state and a steady state. The characteristics of soil water infiltration for the three sampling plots at different soil depths are shown in Figure 2. The water infiltration rate was greater at the soil surface layer 0–20 cm than at deeper layers in the B2 plot, while in the B1 and NV plots, it was smaller at the surface layer than at deeper layers. The initial infiltration rate (*IIR*) was significantly higher in the B2 plot than in both the B1 plot and the NV plot at the soil surface layer from 0 to 20 cm, while the opposite case appeared for deeper soil layers. Meanwhile, the saturated hydraulic conductivity (*Ks*) in the B2 plot increased by 65.5% at the soil surface layer 0–20 cm, compared with the B1 plot. No significant difference in *Ks* among the three plots was found in the deeper soil layers (p > 0.05). Correlation analysis results showed that the soil water movement on the banana plantation was significantly affected by soil physical properties, *IIR* decreasing with increasing bulk density (R^2 = 0.72, p < 0.001) and initial water content (R^2 = 0.47, p < 0.001) and increasing with increasing non-capillary porosity (R^2 = 0.86, p < 0.001) and capillary porosity (R^2 = 0.82, p < 0.001).

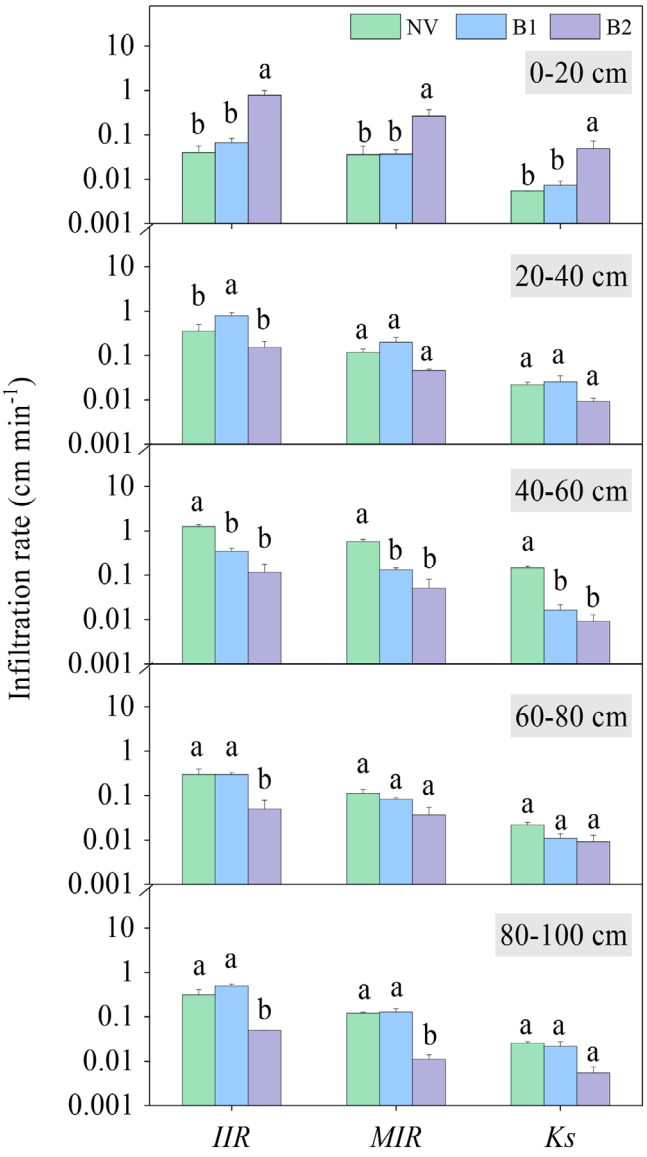

FIGURE 2 Bar graph of infiltration rate (mean ± SE, n = 3) at different soil depths for the three plots (NV, no vegetation. B1, 1-year banana plantation. B2, 4-year banana plantation). *IIR*, initial infiltration rate. M*IR*, mean infiltration rate. *Ks*, saturated hydraulic conductivity. Bars with different lower-case letters (a, b, and c) indicate significant differences at p <0.05 [Colour figure can be viewed at wileyonlinelibrary.com]

The surface soil *Ks* around the banana plants showed an uneven spatial distribution, varying between 0 and 0.34 cm min^{-1}, with a *CV* of 43.4% (Figure 3a). By comparison, the *Ks* was significantly higher near the stem, especially within 50 cm of the stem, compared with further away. Four sensors were installed to monitor the temporal variation of volumetric water content from April to July at different positions (Figure 3b). The results showed that some differences in soil moisture appeared at four sensors: A, B, C, and D. Temporally, the *CV* values were higher at sensor A (6.6%) than at sensors B, C, and D (3.67%, 2.8%, and 3.6%, respectively). The soil moisture of sensors A and B increased clearly after rainfall input, showing that surface soil water can respond rapidly to rainfall input. It should be noted that the

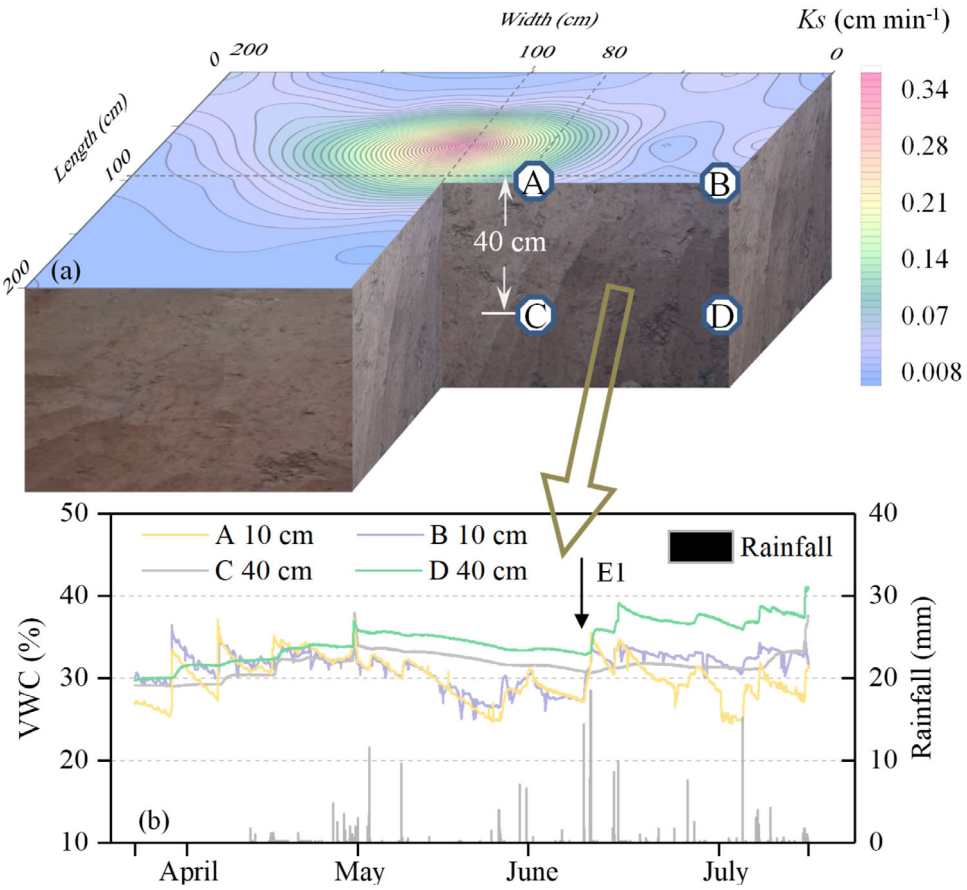

FIGURE 3 (a) Spatial distribution of the soil saturated hydraulic conductivity (*Ks*) and (b) volumetric water content (VWC) at different depths/distances from the banana stem as a response of rainfall events. 'A' sensor was 20 cm away from the stem and 80 cm away from 'B' sensor. 'C' sensor and 'D' sensor are located in 40 cm soil depth below 'A' sensor and 'B' sensor, respectively [Colour figure can be viewed at wileyonlinelibrary.com]

soil moisture at sensor A experienced a large change before and after one rainfall event, and the descending gradient was significantly greater at sensor A than at sensor B. By contrast, the temporal change in the soil moisture in subsurface soil was clearly less than that in surface soil, especially at sensor C. The soil moisture at sensor C was always lower than that at sensor D. After the occurrence of a heavy rainfall event E1, the soil moisture showed a significant increase at sensor D, while a very slight increase was monitored at sensor C.

3.3 | Dyeing patterns in the soil profiles

A total of 24 soil dyeing profiles were sampled in the NV, B1, and B2 plots (eight profiles per plot). The 3-D spatial distributions of the dyeing depth in all three plots were uneven (Figure 4a–c). The dyeing depth curves fluctuated greatly between 0 and 85 cm, for example, the P6 and P8 profiles in the B1 plot and the P6 and P4 profiles in the B2 plot. In all three plots, the dyeing depth of the middle area was deeper than that of the outer area, showing a 'tower' structure. By contrast, the maximum dyeing depth of the B2 plot (>80 cm) was greater than that of the B1 and NV plots (<60 cm). In addition, because banana roots occupied a certain space and hindered staining, low dyeing depths in the centre area were shown, for example, in P6 (B1–P6) of the B1 plot and P6 (B2–P6) of the B2 plot.

The results of preferential flow indices showed some differences among the three plots (Figure 4d–g). The dye coverage (*DC*) of the B2 plot was significantly larger than that of the B1 and NV plots ($p < 0.05$). Similarly, both the CV and the uniform infiltration depth (*UID*) of the B2 plot were significantly larger than those of the other two plots ($p < 0.05$). Moreover, the B2 plot showed a higher preferential flow fraction (*Pf-r*) than the other two plots, though no significant difference was found ($p > 0.05$). These results indicated that the 4-year B2 plot represented a stronger preferential flow than the 1-year B1 plot, and the B1 plot had a slightly stronger preferential flow than NV plot. In addition, the root zone (yellow filled area in Figure 4d–g) showed different values to the non-root zone, indicating that more obvious preferential flow occurred in the root zone than in the non-root zone.

Three typical profiles NV-P4, B1-P5, and B2-P6, respectively from the NV, B1, and B2 plots, were selected in order to evaluate the changes in dyeing patterns (Figure 5). The results showed that preferential flow was dominant, and the soil matrix was bypassed. The dyeing depth was limited to 0–40 cm in the NV plot, and the water infiltration of the deeper soil layer was blocked. Within a width of 80 cm divided into four columns, both the dyeing depth and *DC* of the middle area were slightly larger than those of the outside area. However, the dyeing patterns of the B1 and B2 plots with banana planting were very uneven and significantly different from those of the NV plot. In the 1-year B1 plot, both dyeing depth and *DC* were significantly higher within 40 cm of the stem (depth 60 cm, *DC* 61.6%) than other distance ranges, and the shallowest dyeing depth and *DC* was found far from the stem. The same situation also occurred in the

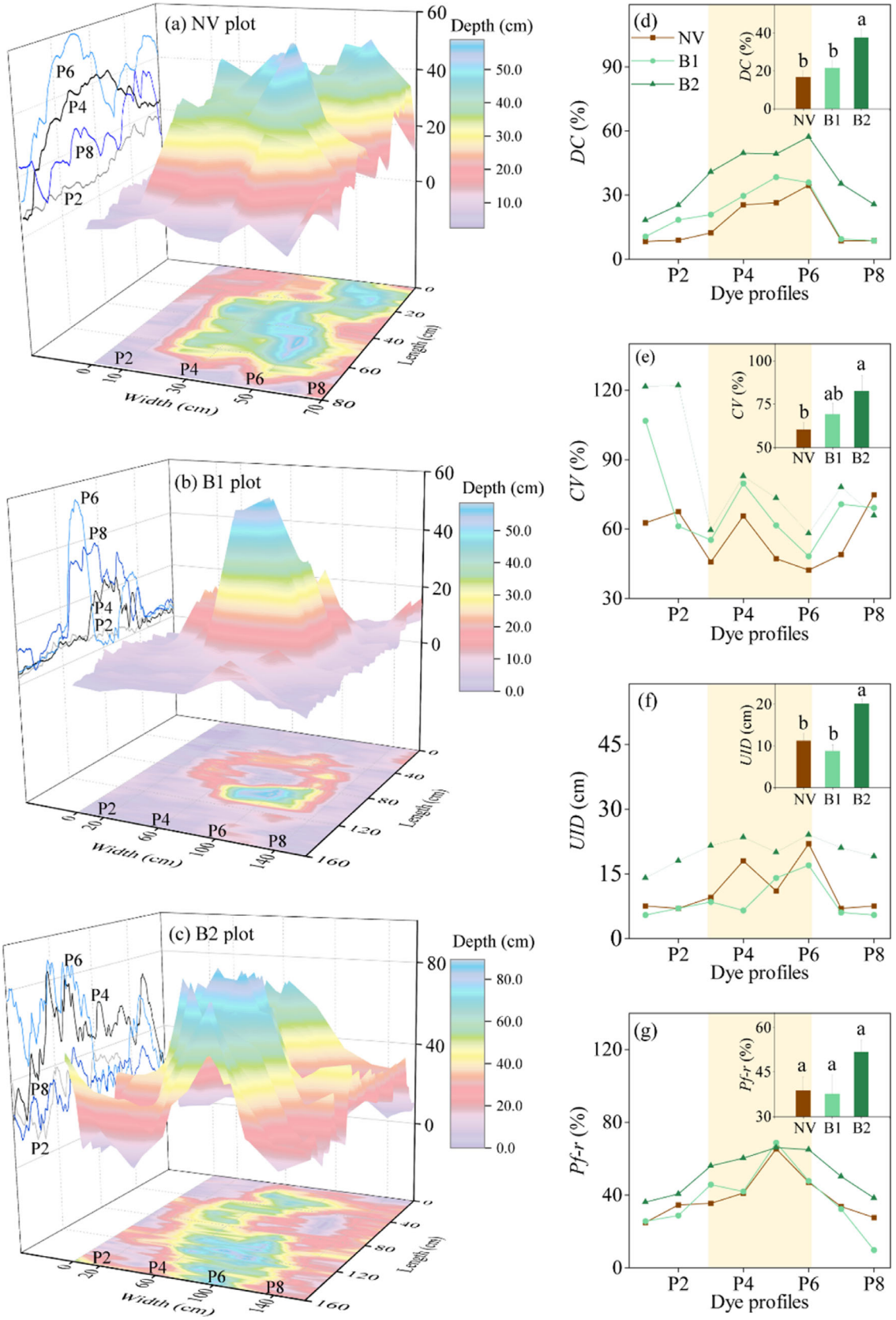

FIGURE 4 Distribution of dyeing depths for the three plots, (a) NV, no vegetation, (b) B1 plot, 1-year banana plantation, (c) B2 plot, 4-year banana plantation). Dye profiles P2, P4, P6 and P8 were marked as the reference profiles. Preferential flow indices of dye profiles were calculated, (d) *DC*: Dye coverage (%), (e) *CV*: Coefficient of variation (%), (f) *UID*: Uniform infiltration depth (cm) and (g) *PF-fr*: Preferential flow fraction (%). The yellow area is the banana root area, and the different lower-case letters (a, b and c) indicate significant difference at $p < 0.05$ [Colour figure can be viewed at wileyonlinelibrary.com]

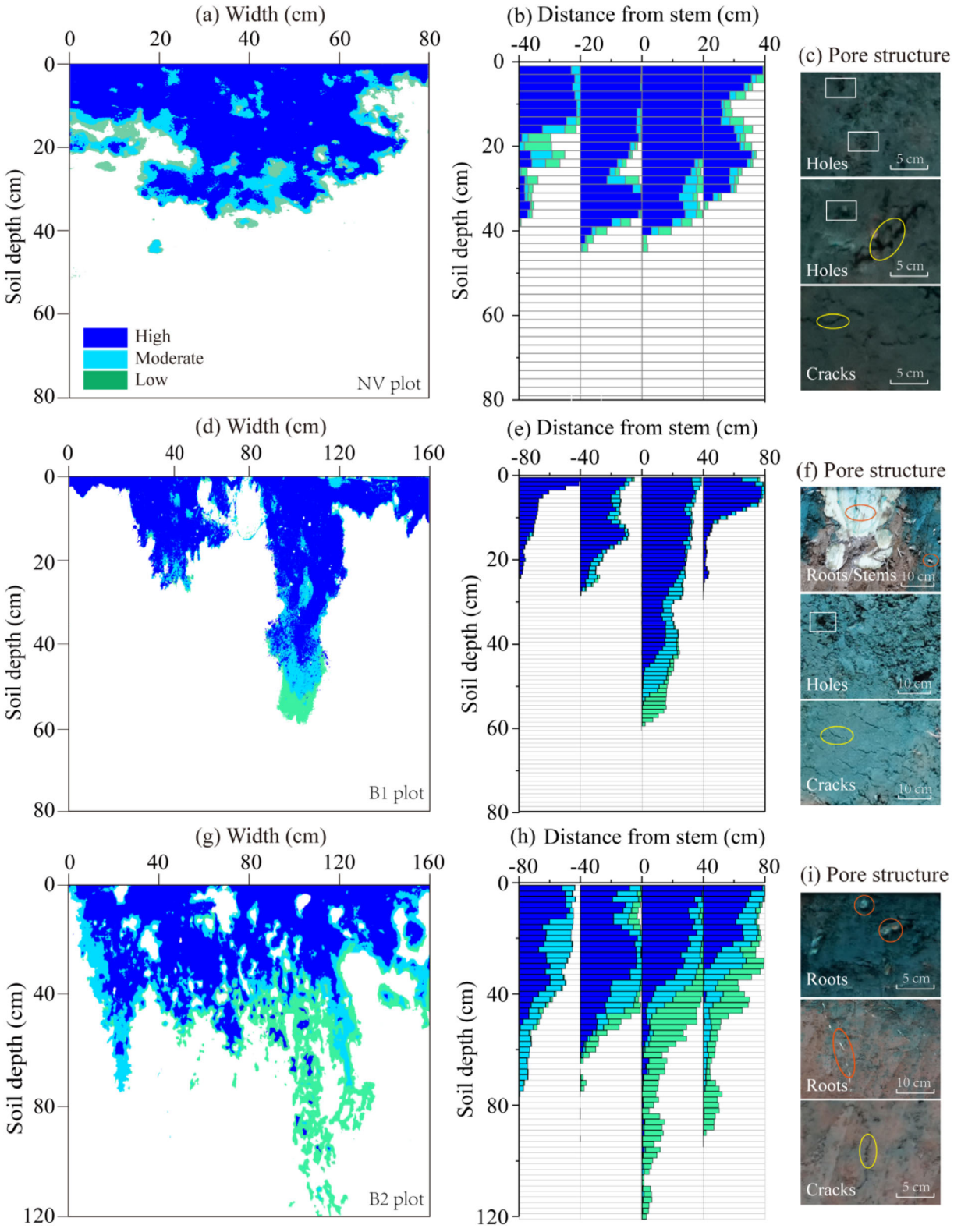

FIGURE 5 (a, d, g) infiltration patterns for vertical soil profiles in the three plots (NV, no vegetation; B1 plot, 1-year banana plantation; B2 plot, 4-year banana plantation). (b, e, h) calculated dyeing area percent (%) in different areas distance from banana stem. (c, f, i) real pore structure of different soil layers. Colour filled areas are classified into dark (high concentration), moderate (moderate concentration) and light (low concentration) [Colour figure can be viewed at wileyonlinelibrary.com]

4-year B2 plot, with a dyeing depth of 120 cm and *DC* 57.6% near the stem, significantly greater than that of the outside area. Thus, the above results indicated that preferential flow showed obvious differences between the root zone and the non-root zone. In addition, the results of different dyeing concentration classifications showed obvious differences in the *DC*. For the B1 and B2 plots, the *DC* with a

high concentration (dark dyeing area) was greater in the shallow soil layer and the area near the stem than in the deeper soil layer and the outside area.

3.4 | Correlation between dyeing area and soil variables

Correlations between the dyeing area and soil physical properties were analyzed (Table 2). A negative correlation between dyeing area and bulk density was found ($r = -0.6$, $p < 0.001$, $n = 87$). The dyeing area was positively correlated with soil porosity ($r = 0.6$, $p < 0.001$, $n = 87$). For dyeing areas of varying concentrations, the high concentration dyeing area has a closer relationship with the soil physical properties (e.g., bulk density) than the low-concentration dyeing area. Moreover, the change in dyeing area was related to the root biomass (RB) on the banana plantation. The dyeing area increased significantly with increasing RB ($r = 0.53$, $p < 0.001$, $n = 35$). The three kinds of root diameter biomass contributed to the dyeing area, indicating that both thick and fine roots are conducive to water flow.

RDA results showed the correlations between dyeing area and soil property as well as the correlations among dyeing area variables or the correlations among soil property variables (Figure 6). The first and second axis explain 39.3% and 4.5% of the variation of relationship between dyeing area variables and soil property variables, respectively. RB was the dominant soil property variables, with the longer vertical projection onto the second axis than BD and other variables. Meanwhile, the dark dyeing area was the dominant dyeing area variable, with the longer vertical projection onto the first axis than other dyeing area variables. A negative relationship was found between BD and dyeing area, with an obtuse angle between vector lines. The dark dyeing area was closely positively correlated with RB, having the longer vector line and the smaller angle. The light dyeing area was closely correlated with non-capillary porosity. The total dyeing area was mostly related to the total soil porosity.

4 | DISCUSSION

4.1 | Differences in soil physical properties

Soil physical properties are the most important factors affecting plant water use and nutrient acquisition and groundwater recharge (Renger et al., 1986). Soil physical properties, affected by land use types, vegetation, topography, and other factors, show spatial variability (Yimer et al., 2006). In the banana plantation, soil physical properties changed significantly with increasing soil depths (Table 1). Lower bulk density,

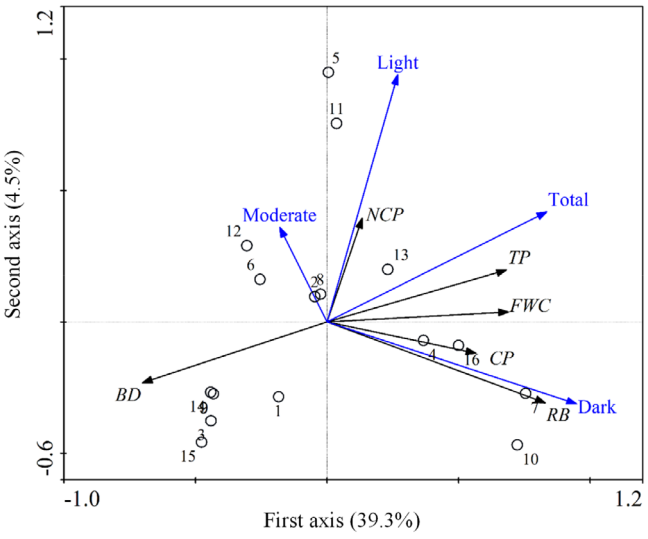

FIGURE 6 Ordination diagram showing the results of RDA of soil property variables and dyeing area variables. Soil property variables refer to *BD*, bulk density; *CP*, capillary porosity; *NCP*, non-capillary porosity; *TP*, total porosity; *FWC*, field water capacity; *RB*, root biomass. Dye variables refer to dark dyeing (high concentration), moderate dyeing (moderate concentration), light dyeing (low concentration) and total dyeing area [Colour figure can be viewed at wileyonlinelibrary.com]

TABLE 2 Correlation coefficients between dyeing area and soil physical properties

Variables	n	Dark-dye	Moderate-dye	Wathet-dye	Total-dye
BD	87	−0.68***	−0.14	−0.39***	−0.60***
NCP	87	0.40**	0.08	0.49***	0.62***
CP	87	0.66***	0.04	0.27*	0.47***
TP	87	0.68***	0.14	0.40***	0.60***
IWC	87	0.57***	0.24*	0.22*	0.51***
FWC	87	0.67***	0.01	0.33**	0.50***
Total-RB	35	0.82***	−0.01	−0.08	0.53***
Thick-RB	35	0.78***	−0.05	−0.2	0.46**
Medium-RB	35	0.57**	−0.11	0.02	0.38
Fine-RB	35	0.67***	−0.01	−0.15	0.42*

Note: Soil physical properties refer to BD, bulk density; NCP, noncapillary porosity; CP, capillary porosity; RB, root biomass; TP, total porosity; IWC, initial water content. Soil hydrological properties refer to FWC, field water capacity. Root systems refer to thick (>3 mm), medium (1–3 mm), fine (<1 mm) and total root biomass. Dye variables refer to dark (high concentration), moderate (moderate concentration), wathet (low concentration) and total dyeing area. Significance test ***, $p < 0.001$; **, $p < 0.01$; *, $p < 0.05$

higher porosity, and field water capacity appeared in the shallow soil layer than deeper soil layers. The extensive plant root, soil fauna, and microbial activity of shallow soil layer can reduce soil compaction (Chen et al., 2018). In addition, surface soil was also subjected to more intense external forces for shallow soil layers, e.g., trampling by human and agricultural machinery (Liu et al., 2016). Consequently, soil non-capillary porosity changes were more pronounced in the shallow soil layers than deeper soil layers, lower value at soil surface 0–20 cm than depth 20–40 cm.

For different land use types in the same area of Xishuangbanna, the soil bulk density of the banana plantations (1.63 g cm^{-3}) was higher than that of rubber (*Hevea brasiliensis*) plantation (1.29 g cm^{-3}) and tea (*Camellia sinensis* L.) plantations (1.26 g cm^{-3}); both capillary porosity and field water capacity were smaller than those of rubber and tea plantations (Zhu et al., 2019). Moreover, long-term continuous cultivation of monoculture banana cropping can significantly change soil physical properties, even degraded soil structure. According to Shen et al. (2018) study, successive banana cropping would also significantly induce the *Fusarium* wilt disease incidence, higher disease incidence for 6-year cropping than 1-year and 2-year. Likewise, Zhong et al. (2015) noted that banana monoculture was not sustainable for clayey and sandy soils in the tropics, and suggested that management decisions for banana production on tropical environment should consider the positive effects of cropping regimes to improve soil quality. Also, continuous maize (*Zea mays* L.), wheat (*Triticum aestivum* L.), and tea (*Camellia sinensis*) cropping all have been proved to be have adverse effects on soil quality and crop yield (Arafat et al., 2019; Lal, 1997; Singh et al., 2014). Therefore, developing sustainable crops planting need to take monoculture planting ages into consideration.

Plant root distribution showed spatial variability, and can improve the nearby soil porosity, aggregate stability and organic matter, and enhance water infiltration (Chandler & Chappell, 2008; Sidle et al., 2006). As described by Yang et al. (2020), a mature banana plant root biomass concentrated in soil depth 0–30 cm (0.64 kg m^{-3}), 4-times - deeper depth 30–80 cm (0.15 kg m^{-3}). Our results showed that the soil bulk density was lower, and soil porosity, and field water capacity were greater in the shallow soil layers than the deeper soil layers in the banana plantation, which was closely related to the banana root systems. Moreover, some differences of soil physical properties were also found in between root zone and non-root zone (Table 1). Soil porosity was higher in the root zone than non-root zone, indicating that banana root systems indeed have improved soil physical properties. In this regard, for many vegetation cover types, for example, coffee (*Coffea arabica* L., var Caturra), pasture, teak (*Tectona grandis*), it has been demonstrated that the soil physical and hydraulic properties around the root systems change significantly from those far away from the root zone (Benegas et al., 2014; Tarafdar & Jungk, 1987). The banana root systems in the B2 plot were stronger, including more living and decayed roots, than those in the B1 plot, however, the soil quality was worse in the B2 plot than B1 plot. Such result should be attributed to the tillage practice of banana plantation, especially little plowing and prolonged trampling being the main causes of soil compaction (Jabro et al., 2009; Liu et al., 2016). Besides, there was no significant difference of the soil physical properties between the B1 plot and the NV plot, which might be attributed to a short crop life and underdeveloped root systems in the B1 plot.

4.2 | Preferential flow and influencing factors

Preferential flow has been shown to dominate compared to matrix flow in some vegetation systems (Benegas et al., 2014; Zhu et al., 2019). In our study, the preferential flow path was well characterized using dye-tracer techniques. Meanwhile, the indices (dyeing depth, dye coverage rate, and preferential flow ratio, etc.) characterized quantitatively the degree of preferential flow (Figure 4). Results indicated that preferential flow in the banana plantation was expected to be stronger than that in open field, which was attributed to the underlying surface soil and vegetation influencing. The wide ranges of preferential flow were successfully captured based on the dyeing area. Corresponding to the dyeing area, the pore types of NV plot are mainly soil holes and cracks, and the preferential flow was induced by soil macropores. The gaps generated by root activity greatly promoted water flow in the B1 and B2 plots (Figure 5c,f,i), and the preferential flow was mainly induced by root systems. One type of preferential flow, 'finger flow', appeared near the banana stems in the B1 plot. The heterogeneous soil tended to form unstable wetting front and then could break into narrow wetting columns or 'fingers' (Kim et al., 2005). Biological factors, microorganisms, and roots activities in the heterogeneous soil could promote the formation of unstable wetting front, thereby affecting soil water flow (Li et al., 2018; Morales et al., 2010). Besides, the interactions between preferential flow and matrix flow were also found based on the moderate and light dyeing area, indicating a water movement shift from the macropores flow to the matrix flow and subsequently a more matrix-dominated flow into the deeper soil layers.

Correlation analysis showed that the dyeing area was negatively correlated with bulk density, and was positively correlated with porosity and root biomass (Table 2). The bulk density was lower in the dyeing area by 0.2 g cm^{-3} than soil non-dyeing area, and the total porosity was greater in the dyeing area by 4.1%. Similarly, Bogner et al. (2010) identified the effect of soil bulk density on the preferential flow in a Norway spruce forest soil, and emphasized that roots considerably promoted the preferential flow. Plant root systems can generate abundant channels for plants to absorb soil water and nutrients, and the root distribution directly affects the transport characteristics and permeability of water and nutrients (Martinez et al., 2008). In this study, some differences of the dyeing patterns between the root zone and the non-root zone were found (Figure 5e,h). In addition, the results of RDA showed that root biomass was the most important factor affecting the dyeing area (Figure 6), suggesting that banana root systems can generate abundant pore channels promoting the preferential flow. The importance of root activity in the soil water flow process was well proved. One of the evidences showed that both the dyeing depth of 4-year B2 plot were significantly deeper than that of NV plot. There is no root distribution in the NV plot, and

consequently, the dyeing depth is limited to the soil layer above 40 cm. The other evidence was that the quantified indices in the root zones of both B1 and B2 plots performed significantly better than that in the non-root zone (Figure 4).

The water flow patterns between the 1-year B1 plot and 4-year B2 plot were different. The preferential flow of the B2 plot was considerably more dominant compared to B1 plot, suggesting that the macropores formed by the developed roots systems of B2 plot enhanced water preferably to the deep soil. According to previous research by Lesturgez et al. (2004), soil physical properties of continuous monoculture cropping are not conducive to rapid water movement. On average, the soil bulk density significantly increased with long planting age, and the porosity also decreased, indicating that the soil quality in the B2 plot tended to be worse than B1 plot. However, the root systems in the B1 plot decreased in the deeper soil layers. Consequently, soil preferential flow paths of B1 plot were limited. Therefore, well-developed root systems can accelerate the process of water transport, and attenuate runoff and soil erosion (Bargués-Tobella et al., 2014; Niemeyer et al., 2014). Besides, it should be noted that preferential flow may result in fertilizer and pesticide transport to deeper layers. Banana is a crop with the high demand of water and fertilizer, and long-term planting banana will accumulate abundant chemical residues. The studies in Venezuela by Olivares et al. (2021) and Paredes et al. (2021) establish that banana in areas of great commercial importance is a crop with an important demand for water and chemical products for conventional management, with the majority of plantations more than 10 years-age. Long-term banana planting will accumulate abundant chemical residues, which generates inconveniences in the filtration and movement of water in the soil coupled with the absence of soil and water conservation practices in the plots. Hence, the improvement of irrigation depending on the planting age of the banana plantation is strictly necessary to avoid infiltration problems of the underground water.

4.3 | Effect of soil physical properties on water infiltration

Soil water infiltration performance has a positive effect on reducing surface runoff, and is an important basis for evaluating soil erosion resistance capacity (Ellison, 1945). Both soil physical properties and plant root systems affect the soil water infiltration (Chen et al., 2019). In this study, negative correlations between infiltration rate and soil bulk density and initial water content, positive correlations between infiltration rate and soil porosity were found, respectively. An investigation by Campos et al. (2020) established that soil physical properties in banana plantations of lacustrine soils in Venezuela do not favor the rapid water movement, such was the case of the high values of bulk density observed in some plots are associated with their lake origin. According to our soil physical property data, 4-year B2 plot had greater bulk density, less capillary porosity, and more non-capillary porosity than 1-year B1 plot. Some differences of soil water infiltration rate among the three different sampling plots were also found. At the soil surface layer 0–20 cm, water infiltration was significantly faster in the B2 plot than B1 plot (Figure 2). The faster infiltration in the B2 plot was potentially induced by the non-capillary porosity, because B2 plot had higher non-capillary porosity (4.7%) than B1 plot (3.5%). Moreover, the initial water content positively determines soil water potential, which has a negative effect on water absorbing, the more initial water content, the slower infiltration rate (Liu et al., 2019). In this study, the initial water content was lower in the B2 plot (18.5%) than B1 plot (25.0%), which also could accelerate water infiltration. Besides, at the subsurface layers 20–60 cm, the infiltration rate of B1 plot was higher than that of B2 plot, different from the soil surface layer. Meanwhile, the *Ks* decreased with increasing soil depths in the B2 plot, contrary to the B1 plot (Figure 3). Previous studies of soil hydraulic properties in the forest, pasture, and agricultural land use types also showed similar variation (Zimmermann et al., 2006). For example, Hao et al. (2019) stated that the *Ks* was higher in bamboo forests and tea plantations than native forest in the surface soil layer; native forest had higher *Ks* than bamboo and tea in the deeper soil. The surface soil is disturbed by external forces more than the subsurface soil, and the soil physical properties in the root zone are different from those in the non-root zone, thus the water infiltration varies greatly among different soil depths and land use types (Klos et al., 2014).

Plant root systems, embedding, entangling and enwrapping in soil, have been shown to improve soil porosity and accelerate water infiltration (Jiang et al., 2019). In this study, the spatial distribution of *Ks* around the banana stem showed that *Ks* value near the stem was higher than that far away (Figure 4). Banana root systems concentrated in surface soil near the stem, thus, contribute to water infiltration. Similar results to ours were noted by Chandler & Chappell (2008) who also found similar spatial distribution of *Ks* under an isolated oak (*Quercus robur*) canopy in northwest England. Moreover, the temporal variation of VWC was monitored, and the sharp increase of VWC in sensors A and B shows that the surface soil water was very responsive. The *Ks* value was higher at sensor A than sensor B, therefore, the decreasing gradient of VWC was greater at sensor A than sensor B. Given that the macropore produced by plant roots could provide channels for the rapid water infiltration (Wine et al., 2012), the drainage capacity is greater in the root zone than the non-root zone. In the banana plantations, the non-capillary porosity in the root zone is significantly higher than that of the non-root zone (Table 1), indicating that the root zone is more conducive to soil water infiltration. Therefore, the VWC at sensor C in the root zone was expected to be lower than that of sensor D in the non-root zone. These findings suggested that soil water infiltration capacity was significantly influenced by soil physical properties and root systems in the banana plantations.

5 | CONCLUSIONS

Soil water flow behaviour in the banana plantation and the effect of soil physical properties on water transport were well quantified using the high-resolution dyeing technique at the plot scales. 3-D spatial distributions of the dyeing depth showed uneven water flow pattern with the root zone had deeper water flow, while the non-root zone

had shallower water flow. Preferential flow was the main mechanism of soil water transport in the banana plantation, and was significantly affected by soil bulk density, porosity, and banana root systems. The downward water infiltration could be weakened by high soil bulk density, but at the same time which could be enhanced by the high non-capillary porosity and root biomass. Thereby, the saturated hydraulic conductivity decreased with the increasing distance from the banana stem, determined by pore channels from root systems. The results of RDA showed that banana root biomass was the major factor influencing the dyeing area, followed by soil porosity. By comparison, both the soil surface infiltration and the preferential flow of B2 plot were stronger than that of B1 plot, though the bulk density of B2 plot was higher. Such result was attributed to the root systems of B2 plot that were more developed than that of B1 plot, and a large number of pore channels formed around the root systems promoted the preferential flow. Overall, the banana root system was the most important factor affecting soil water flow behaviour. Besides, it should be noted that soil structure decreased with the increasing planting age. Hence, the improvement of monoculture planting duration in the banana plantations is essential to avoid soil structure degradation.

ACKNOWLEDGMENTS

We deeply thank Mr. Liu MN for his help in the fields. We also thank the Xishuangbanna Station for Tropical Rainforest Ecosystem Studies and the Central Laboratory of XTBG for their help. This research was supported by the Natural Science Foundation of Yunnan Province (202101AS070010, 202101AT070056, 202001AU070136, 2018FB076 and 2018FB043), the National Natural Science Foundation of China (41701029 and 32001221), and the Natural Science Excellent Youth Foundation of Yunnan Province (2019FI011).

CONFLICT OF INTEREST

The authors declare that they have no known competing financial interests or personal relationships that could have appeared to influence the work reported in this paper.

DATA AVAILABILITY STATEMENT

The data that support the findings of this study are openly available in [repository name e.g "figshare"] at http://doi.org/[doi], reference number [reference number].

ORCID

Wenjie Liu https://orcid.org/0000-0002-9918-3462

REFERENCES

Allaire, S. E., Roulier, S., & Cessna, A. J. (2009). Quantifying preferential flow in soils: A review of different techniques. *Journal of Hydrology*, *378*, 179–204. https://doi.org/10.1016/j.jhydrol.2009.08.013

Arafat, Y., Tayyab, M., Khan, M. U., Chen, T., Amjad, H., Awais, S., Lin, X. M., Lin, W. X., & Lin, S. (2019). Long-term monoculture negatively regulates fungal community composition and abundance of tea orchards. *Agronomy*, *9*(8), 466. https://doi.org/10.3390/agronomy9080466

Bargués-Tobella, A., Reese, H., Almaw, A., Bayala, J., Malmer, A., Laudon, H., & Ilstedt, U. (2014). The effect of trees on preferential flow and soil infiltrability in an agroforestry parkland in semiarid Burkina Faso. *Water Resource Research*, *50*(4), 3342–3354. https://doi.org/10.1002/2013WR015197

Benegas, L., Ilstedt, U., Roupsard, O., Jones, J., & Malmer, A. (2014). Effects of trees on infiltrability and preferential flow in two contrasting agroecosystems in Central America. *Agriculture, Ecosystems & Environment*, *183*, 185–196. https://doi.org/10.1016/j.agee.2013.10.027

Beven, K., & Germann, P. (2013). Macropores and water flow in soils revisited. *Water Resource Research*, *49*(6), 3071–3092. https://doi.org/10.1002/wrcr.20156

Bodhinayake, W., Si, B. C., & Noborio, K. (2004). Determination of hydraulic properties insloping landscapes from tension and double-ring infiltrometers. *Vadose Zone Journal*, *3*(3), 964–970. https://doi.org/10.2113/3.3.964

Bogner, C., Gaul, D., Kolb, A., Schmiedinger, I., & Huwe, B. (2010). Investigating flow mechanisms in a forest soil by mixed-effects modelling. *European Journal of Soil Science*, *61*(6), 1079–1090. https://doi.org/10.1111/j.1365-2389.2010.01300.x

Bouma, J., Jongerius, A., Boersma, O., Jager, A., & Schoonderbeek, D. (1977). The function of different types of macropores during saturated flow through four swelling soil horizons. *Soil Science Society of America Journal*, *41*, 945–950. https://doi.org/10.2136/sssaj1977.03615995004100050028x

Bromley, J., Brouwer, J., Barker, A. P., Gaze, S. R., & Valentine, C. (1997). The role of surface water redistribution in an area of patterned vegetation in a semi-arid environment, South-West Niger. *Journal of Hydrology*, *198*(1–4), 1–29. https://doi.org/10.1016/S0022-1694(96)03322-7

Campos, O., Araya-Alman, M., Acevedo-Opazo, C., Cañete-Salinas, P., Rey, J. C., Lobo, D., & Landa, B. (2020). Relationship between soil properties and Banana productivity in the two main cultivation areas in Venezuela. *Journal of Soil Science and Plant Nutrition*, *20*(3), 2512–2524. https://doi.org/10.1007/s42729-020-00317-8

Chandler, K. R., & Chappell, N. A. (2008). Influence of individual oak (*Quercus robur*) trees on saturated hydraulic conductivity. *Forest Ecology and Management*, *256*(5), 1222–1229. https://doi.org/10.1016/j.foreco.2008.06.033

Chen, C. F., Liu, W. J., Wu, J. N., & Jiang, X. J. (2018). Spatio-temporal variations of carbon and nitrogen in biogenic structures of two fungus-growing termites (M. *annandalei* and O. *yunnanensis*) in the Xishuangbanna region. *Soil Biology and Biochemistry*, *117*, 125–134. https://doi.org/10.1016/j.soilbio.2017.11.018

Chen, C. F., Liu, W. J., Wu, J. E., Jiang, X. J., & Zhu, X. A. (2019). Can intercropping with the cash crop help improve the soil physico-chemical properties of rubber plantations? *Geoderma*, *335*, 149–160. https://doi.org/10.1016/j.geoderma.2018.08.023

Danielson, R. E., & Sutherland, P. L. (1986). Porosity. In A. Klute (Ed.), *Methods of soil analysis. Part 1. Physical and mineralogical methods. Agronomy monograph No. 9. American Society of Agronomy, Soil Science Society of America* (pp. 443–461). Madison, WI: Soil Science Society of America.

Ellison, W. D. (1945). Some effects of raindrops and surface–flow on soil erosion and infiltration. *Eos, Transactions American Geophysical Union*, *26*(3), 415–429. https://doi.org/10.1029/TR026i003p00415

Flury, M., Fluhler, H., Jury, M. A., & Leuenberger, J. (1994). Susceptibility of soils to preferential flow of water: A field study. *Water Resource Research*, *30*(7), 1945–1954. https://doi.org/10.1029/94WR00871

Gabarrón, M., Faz, A., & Acosta, J. A. (2018). Use of multivariable and redundancy analysis to assess the behavior of metals and arsenic in urban soil and road dust affected by metallic mining as a base for risk assessment. *Journal of Environmental Management*, *206*, 192–201. https://doi.org/10.1016/j.jenvman.2017.10.034

Gazis, C., & Feng, X. (2004). A stable isotope study of soil water: Evidence for mixing and preferential flow paths. *Geoderma*, *119*(1–2), 97–111. https://doi.org/10.1016/S0016-7061(03)00243-X

Ghodrati, M., & Jury, W. A. (1990). A field study using dyes to characterize preferential flow of water. *Soil Science Society of America Journal*, *54*, 1558–1563. https://doi.org/10.2136/sssaj1990.03615995005400060008x

Hardie, M. A., Cotching, W. E., Doyle, R. B., Holz, G., Lisson, S., & Mattern, K. (2011). Effect of antecedent soil moisture on preferential flow in a texture-contrast soil. *Journal of Hydrology*, *398*(3), 191–201. https://doi.org/10.1016/j.jhydrol.2010.12.008

Hao, M. Z., Zhang, J. C., Meng, M. J., Chen, H. Y. H., Guo, X. P., Liu, S. L., & Ye, L. X. (2019). Impacts of changes in vegetation on saturated hydraulic conductivity of soil in subtropical forests. *Scientific Reports*, *9*, 8372. https://doi.org/10.1038/s41598-019-44921-w

Martinez, E., Fuentes, J. P., Silva, P., Valle, S., & Acevedo, E. (2008). Soil physical properties and wheat root growth as affected by no-tillage and conventional tillage systems in a Mediterranean environment of Chile. *Soil & Tillage Research*, *99*(2), 232–244. https://doi.org/10.1016/j.still.2008.02.001

Jabro, J. D., Stevens, W. B., Evans, R. G., & Iversen, W. M. (2009). Tillage effects on physical properties in two soils of the northern Great Plains. *Applied Engineering In Agriculture*, *25*, 377–382. https://doi.org/10.13031/2013.26889

Jiang, X. J., Chen, C. F., Zhu, X. A., Zakaria, S., Singha, A. K., Zhang, W. J., Zeng, H. H., Yuan, Z. Q., He, C. G., Yu, S. Q., & Liu, W. J. (2019). Use of dye infiltration experiments and HYDRUS-3D to interpret preferential flow in soil in a rubber-based agroforestry systems in Xishuangbanna, China. *Catena*, *178*, 120–131. https://doi.org/10.1016/j.catena.2019.03.015

Jiang, X. J., Liu, W. J., Chen, C. F., Liu, J. Q., Yuan, Z. Q., Jin, B. C., & Yu, X. Y. (2018). Effects of three morphometric features of roots on soil water flow behavior in three sites in China. *Geoderma*, *320*, 161–171. https://doi.org/10.1016/j.geoderma.2018.01.035

Jiang, X., Liu, X., Wang, E., Li, X. G., Sun, R., & Shi, W. (2015). Effects of tillage pan on soil water distribution in alfalfa-corn crop rotation systems using a dye tracer and geostatistical methods. *Soil & Tillage Research*, *150*, 68–77. https://doi.org/10.1016/j.still.2015.01.009

Jørgensen, P. R., Hoffmann, M., Kistrup, J. P., Bryde, C., Bossi, R., & Villholth, K. G. (2002). Preferential flow and pesticide transport in a clay-rich till: Field, laboratory, and modeling analysis. *Water Resource Research*, *38*(11), 28-1–28-15. https://doi.org/10.1029/2001WR000494

Kim, Y., Darnault, C. J. G., Bailey, N. O., Parlange, J., & Steenhuis, T. S. (2005). Equation for describing solute transport in field soils with preferential flow paths. *Soil Science Society of America Journal*, *69*, 291–300. https://doi.org/10.2136/sssaj2005.0291a

Klos, P. Z., Chain-Guadarrama, A., Link, T. E., Finegan, B., Vierling, L. A., & Chazdon, R. (2014). Throughfall heterogeneity in tropical forested landscapes as a focal mechanism for deep percolation. *Journal of Hydrology*, *519*, 2180–2188. https://doi.org/10.1016/j.jhydrol.2014.10.004

Lal, R. (1997). Long-term tillage and maize monoculture effects on a tropical Aalfisol in western Nigeria. I. Crop yield and soil physical properties. *Soil & Tillage Research*, *42*(3), 145–160. https://doi.org/10.1016/S0167-1987(97)00006-8

Lesturgez, G., Poss, R., Hartmann, C., Bourdon, E., Noble, A., & Ratana-Anupap, S. (2004). Roots of stylosanthes hamata create macropores in the compact layer of a sandy soil. *Plant and Soil*, *260*(1–2), 101–109. https://doi.org/10.1023/B:PLSO.0000030184.24866.aa

Li, B. T., Pales, A. R., Clifford, H. M., Kupis, S., Hennessy, S., Liang, W. Z., Moysey, S., Powell, B., Finneran, K. T., & Darnault, C. J. G. (2018). Preferential flow in the vadose zone and interface dynamics: Impact of microbial exudates. *Journal of Hydrology*, *558*, 72–89. https://doi.org/10.1016/j.jhydrol.2017.12.065

Lipiec, J., Kuś, J., Słowińska-Jurkiewicz, A., & Nosalewicz, A. (2006). Soil porosity and water infiltration as influenced by tillage methods. *Soil & Tillage Research*, *89*, 210–220. https://doi.org/10.1016/j.still.2005.07.012

Liu, W. J., Zhu, C. J., Wu, J. E., & Chen, C. F. (2016). Are rubber-based agroforestry systems effective in controlling rain splash erosion? *Catena*, *147*, 16–24. https://doi.org/10.1016/j.catena.2016.06.034

Liu, Y., Cui, Z., Huang, Z., López-Vicente, M., & Wu, G. L. (2019). Influence of soil moisture and plant roots on the soil infiltration capacity at different stages in arid grasslands of China. *Catena*, *182*, 104147. https://doi.org/10.1016/j.catena.2019.104147

Ludwig, J. A., Wilcox, B. P., Breshears, D. D., Tongway, D. J., & Imeson, A. C. (2005). Vegetation patches and runoff-erosion as interacting ecohydrological processes in semiarid landscapes. *Ecology*, *86*, 288–297. https://doi.org/10.1890/03-0569

Morales, V. L., Parlange, J. Y., & Steenhuis, T. S. (2010). Are preferential flow paths perpetuated by microbial activity in the soil matrix? A review. *Journal of Hydrology*, *393*, 29–36. https://doi.org/10.1016/j.jhydrol.2009.12.048

Niemeyer, R. J., Fremier, A. K., Heinse, R., Chávez, W., & Declerck, F. A. J. (2014). Woody vegetation increases saturated hydraulic conductivity in dry tropical Nicaragua. *Vadose Zone Journal*, *13*(1), 1–11. https://doi, https://doi.org/10.2136/vzj2013.01.0025

Öhrström, P., Persson, M., Albergel, J., Zante, P., Nasri, S., Berndtsson, R., & Olsson, J. (2002). Field-scale variation of preferential flow as indicated from dye coverage. *Journal of Hydrology*, *257*(1–4), 164–173. https://doi.org/10.1016/S0022-1694(01)00537-6

Olivares, B., Rey, J. C., Lobo, D., Navas-Cortés, J. A., Gómez, J. A., & Landa, B. B. (2021). Fusarium wilt of bananas: A review of agro-environmental factors in the venezuelan production system affecting its development. *Agronomy*, *11*(5), 986. https://doi.org/10.3390/agronomy11050986

Paredes, F., Orlando, B. O., Rey, J., Lobo, D., & Galvis-Causil, S. (2021). The relationship between the normalized difference vegetation index, rainfall, and potential evapotranspiration in a banana plantation of Venezuela. *SAINS TANAH - Journal of Soil Science and Agroclimatology*, *18*(1), 58–64. https://doi.org/10.20961/stjssa.v18i1.50379

People's Government of Xishuangbanna (2018). Notice of the Office of the People's Government of Xishuang Banner on printing and distributing the guiding opinions on the development of the banana industry in Xishuangbanna. Xishuangbanna: The Government Office, No. 13. https://www.xsbn.gov.cn/192.news.detail.dhtml?news_id=48497

Renger, M., Strebel, O., Wessolek, G., & Duynisveld, W. H. M. (1986). Evapotranspiration and groundwater recharge–a case study for different climate, crop patterns, soil properties and groundwater depth conditions. *Zeitschrift für Pflanzenernährung und Bodenkunde*, *149*(4), 371–381. https://doi.org/10.1002/jpln.19861490403

Reynolds, W. D., & Elrick, D. E. (1990). Ponded infiltration from a single ring: I. analysis of steady flow. *Soil Science Society of America Journal*, *54*(5), 1233–1241. https://doi.org/10.2136/sssaj1990.03615995005400050006x

Shen, Z. Z., Penton, C. R., Lv, N. N., Xue, C., Yuan, X. F., Ruan, Y. Z., Li, R., & Shen, Q. R. (2018). Banana fusarium wilt disease incidence is influenced by shifts of soil microbial communities under different monoculture spans. *Microbial Ecology*, *75*, 739–750. https://doi.org/10.1007/s00248-017-1052-5

Sidle, R. C., Ziegler, A. D., Negishi, J. N., Nik, A. R., Siew, R. Y., & Turkelboom, F. (2006). Erosion processes in steep terrain—Truths, myths, and uncertainties related to forest management in Southeast Asia. *Forest Ecology and Management*, *224*(1–2), 199–225. https://doi.org/10.1016/j.foreco.2005.12.019

Singh, A., Phogat, V. K., Dahiya, R., & Batra, S. D. (2014). Impact of long-term zero till wheat on soil physical properties and wheat productivity under rice–wheat cropping system. *Soil & Tillage Research*, *140*, 98–105. https://doi.org/10.1016/j.still.2014.03.002

Tarafdar, J. C., & Jungk, A. (1987). Phosphatase activity in the rhizosphere and its relation to the depletion of soil organic phosphorus. *Biology and Fertility of Soils*, *3*(4), 199–204. https://doi.org/10.1007/BF00640630

Van Schaik, N. (2009). Spatial variability of infiltration patterns related to site characteristics in a semi-arid watershed. *Catena*, *78*(1), 36–47. https://doi.org/10.1016/j.catena.2009.02.017

Wang, X. B., Cai, D. X., Hoogmoed, W. B., Oenema, O., & Perdok, U. D. (2007). Developments in conservation tillage in rainfed regions of North China. *Soil & Tillage Research*, *93*(2), 239–250. https://doi.org/10.1016/j.still.2006.05.005

Weiler, M., & Hannes, F. (2004). Inferring flow types from dye patterns in macroporous soils. *Geoderma*, *120*(1–2), 137–153. https://doi.org/10.1016/j.geoderma.2003.08.014

Wine, M. L., Ochsner, T. E., Sutradhar, A., & Pepin, R. (2012). Effects of eastern redcedar encroachment on soil hydraulic properties along Oklahoma's grassland-forest ecotone. *Hydrological Processes*, *26*(11), 1720–1728. https://doi.org/10.1002/hyp.8306

Yang, B., Zhang, W. J., Meng, X. J., Singh, A. K., Zakari, S., Song, L., & Liu, W. J. (2020). Effects of a funnel-shaped canopy on rainfall redistribution and plant water acquisition in a banana (*Musa spp*.) plantation. *Soil & Tillage Research*, *203*, 104686. https://doi.org/10.1016/j.still.2020.104686

Yimer, F., Ledin, S., & Abdelkadir, A. (2006). Soil property variations in relation to topographic aspect and vegetation community in the south-eastern highlands of Ethiopia. *Forest Ecology and Management*, *232*(1–3), 90–99. https://doi.org/10.1016/j.foreco.2006.05.055

Zhang, Z., Xu, E., & Zhang, H. (2021). Complex network and redundancy analysis of spatial–temporal dynamic changes and driving forces behind changes in oases within the Tarim Basin in northwestern China. *Catena*, *201*, 105216. https://doi.org/10.1016/j.catena.2021.105216

Zhong, S., Zeng, H. C., & Jin, Z. Q. (2015). Soil microbiological and biochemical properties as affected by different long–term banana–based rotations in the tropics. *Pedosphere*, *25*(6), 868–877. https://doi.org/10.1016/S1002-0160(15)30067-9

Zhu, X. A., Chen, C. F., Wu, J. E., Yang, J. B., Zhang, W. J., Zou, X., Liu, W. J., & Jiang, X. J. (2019). Can intercrops improve soil water infiltrability and preferential flow in rubber-based agroforestry system? *Soil & Tillage Research*, *191*, 327–339. https://doi.org/10.1016/j.still.2019.04.017

Zimmermann, B., Elsenbeer, H., & De Moraes, J. M. (2006). The influence of land-use changes on soil hydraulic properties: Implications for runoff generation. *Forest Ecology and Management*, *222*, 29–38. https://doi.org/10.1016/j.foreco.2005.10.070

How to cite this article: Zhang, W., Zhu, X., Ji, S., Chen, C., Zeng, H., Zou, X., Yang, B., Jiang, X., & Liu, W. (2022). Soil water movement differences relating to banana (*Musa nana* Lour.) plantation regime. *Land Degradation & Development*, 1–15. https://doi.org/10.1002/ldr.4264